

Proton Coupled Electron Transfer and Redox-Active Tyrosine Z in the Photosynthetic Oxygen-Evolving Complex

James M. Keough, David L. Jenson, Ashley N. Zuniga, and Bridgette A. Barry*

School of Chemistry and Biochemistry and the Petit Institute for Bioengineering and Bioscience, Georgia Institute of Technology, Atlanta, Georgia 30332, United States

ABSTRACT: Proton coupled electron transfer (PCET) reactions play an essential role in many enzymatic processes. In PCET, redox-active tyrosines may be involved as intermediates when the oxidized phenolic side chain deprotonates. Photosystem II (PSII) is an excellent framework for studying PCET reactions, because it contains two redox-active tyrosines, YD and YZ, with different roles in catalysis. One of the redox-active tyrosines, YZ, is essential for oxygen evolution and is rapidly reduced by the manganese-catalytic site. In this report, we investigate the mechanism of YZ PCET in oxygen-evolving PSII. To isolate YZ[•] reactions, but retain the manganese–calcium cluster, low temperatures were used to block the oxidation of the metal cluster, high microwave powers were used to saturate the YD[•] EPR signal, and YZ[•] decay kinetics were measured with EPR spectroscopy. Analysis of the pH and solvent isotope dependence was performed. The rate of YZ[•] decay exhibited a significant solvent isotope effect, and the rate of recombination and the solvent isotope effect were pH independent from pH 5.0 to 7.5. These results are consistent with a rate-limiting, coupled proton electron transfer (CPET) reaction and are contrasted to results obtained for YD[•] decay kinetics at low pH. This effect may be mediated by an extensive hydrogen-bond network around YZ. These experiments imply that PCET reactions distinguish the two PSII redox-active tyrosines.

In this article, EPR spectroscopy is used to investigate YZ PCET reactions in PSII. PSII catalyzes the light driven oxidation of water at a Mn₄CaO₅-containing oxygen-evolving center (OEC). The transmembrane electron transfer pathway involves four chlorophylls (chl), two pheophytins, two plastoquinones, and two redox-active tyrosines, YD and YZ (Figure 1A). Four flashes are required to produce oxygen from water. The OEC cycles among five S_n states, where n refers to the number of oxidizing equivalents stored.¹ YD and YZ^{2,3} are located with approximate C₂ symmetry in the reaction center.^{4,5} These tyrosine residues are equidistant from the chl donor, P₆₈₀, and are active in PCET reactions but play different roles in catalysis. YZ, Y161 of the D1 polypeptide, is essential for oxygen evolution.^{6,7} YD, Y160 of the D2 polypeptide,^{8,9} is not essential for catalysis but may be involved in assembly of the OEC.¹⁰ There are other kinetic and energetic differences between the two tyrosines.¹¹ For example, YD forms a more stable radical and is easier to oxidize.^{7,12} As shown in B and C of Figure 1, the placement of the OEC and neighboring amino acid side chains distinguishes the two redox-active tyrosines. In particular,

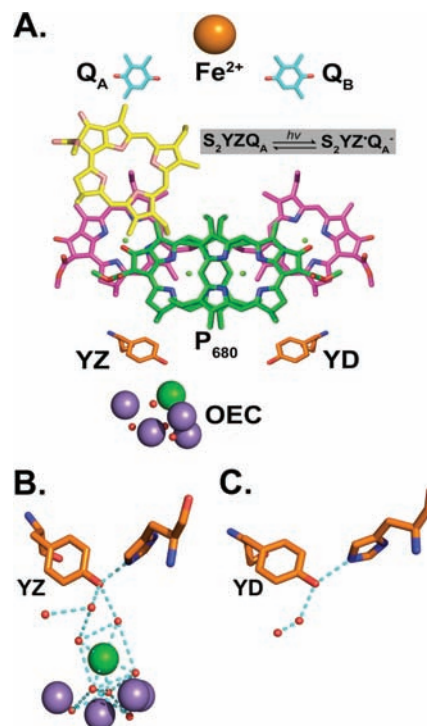


Figure 1. (A) Illustration of the PSII electron transfer pathway, using representations of cofactors. After a saturating flash to a dark-adapted sample at 190 K, recombination occurs between YZ[•] and Q_A⁻ in the OEC S₂ state. From ref 5, hydrogen-bonding environment of (B) YZ (Y161D1), showing interactions (cyan dashed lines) with predicted water molecules and H190D1 and of (C) YD (Y160D2), showing interactions with predicted water molecules and H189D2.⁵ Oxygen atoms are orange, manganese ions are purple, and the calcium ion is green. Hydrogen bonds were predicted using a polar contact function with an edge distance of 3.2 Å and a center distance of 3.6 Å (*The Pymol Molecular Graphics System*, version 1.3, Schrödinger, LLC). (B) and (C) were derived from the 1.9 Å structure from *Thermosynechococcus vulcanus* (3ARC).⁵

the OEC calcium ion is located 5 Å from YZ, but over 20 Å from YD (Figure 1). An extensive set of hydrogen bonds, which link the OEC site and YZ, is predicted. As shown in the 1.9 Å PSII structure (B and C of Figure 1), hydrogen bonding helps to distinguish YZ and YD.⁵

Received: May 4, 2011

Published: June 29, 2011

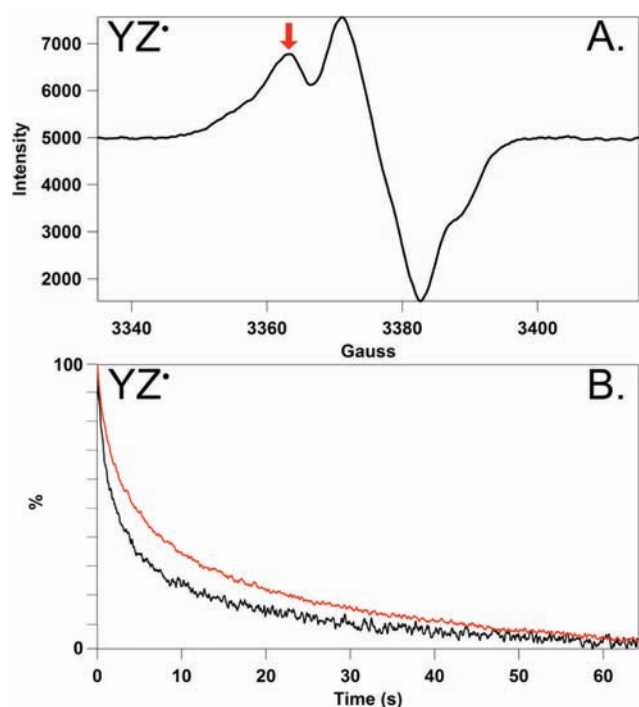


Figure 2. (A) Representative EPR spectrum of the S_2YZ^\bullet state at 190 K and p^1H 6.5. The spectrum was acquired under red-filtered illumination. The red arrow shows the magnetic field used to monitor kinetics. (B) Representative EPR transients reflecting the decay of YZ^\bullet at p^1H 6.5 (black) and p^2H 6.5 (red) at 190 K. PSII was isolated from market spinach.¹³ The average oxygen evolution rate was $600 \mu\text{mol O}_2/\text{mg chl}\cdot\text{h}$.¹⁴ The samples were solvent exchanged by repeated centrifugation at $100,000g$ in a $^1\text{H}_2\text{O}$ or $^2\text{H}_2\text{O}$ (99% Cambridge Isotopes, Andover, MA) buffer containing 0.4 M sucrose, 15 mM NaCl, and 50 mM buffer at each of the following pL values: pL 5.0 (succinate), 5.5 (succinate), 6.0 (2-(*N*-morpholino)ethanesulfonic acid, MES), 6.5 (MES), 7.0 (4-(2-hydroxyethyl)-1-piperazineethanesulfonic acid, HEPES), 7.5 (HEPES). Samples were stored at -70°C . The pL is reported as the uncorrected meter reading.¹⁵ After a 20-min dark adaptation to trap the S_1 state, samples were illuminated with red-filtered light ($600 \mu\text{mol photons}/\text{m}^2\cdot\text{s}$, Dolan Jenner Industries, Boxborough, MA) with $500 \mu\text{M}$ potassium ferricyanide at 190 K to generate the S_2 state. Transient data at constant field were obtained following a 532 nm flash from a Continuum (Santa Clara, CA) Surelite III Nd:YAG laser. The laser intensity was $40 \text{ mJ}/\text{cm}^2$, and the beam was expanded with a cylindrical lens. Transient data, associated with $S_2YZ^\bullet Q_A^-$ decay, are averages from 3–5 samples; 15 transients were recorded per sample. EPR analysis was conducted on a Bruker (Billerica, MA) EMX spectrometer equipped with a Bruker ER 4102ST cavity and Bruker ER 4131VT temperature controller. EPR parameters in (A): frequency: 9.47 GHz, power: 0.638 mW, modulation amplitude: 2 G, conversion time: 40.960 ms, time constant: 163.840 ms, sweep time: 20.972 s. EPR parameters in (B): magnetic field: 3360 G, microwave frequency: 9.47 GHz, power: 101 mW, modulation amplitude: 5 G, conversion: 20.48 ms, time constant: 164 ms. An offset, recorded from 10 s of data before the flash, was subtracted. Transients were normalized to 100% at time zero. To show that the expected YZ^\bullet hyperfine splitting is observed, the microwave power and modulation amplitude in (A) were reduced in comparison to those in (B).

YZ mediates electron transfer between the primary chl donor, P_{680} , and the OEC.¹⁶ Photoexcitation of PSII produces a chl cation radical, P_{680}^+ , which oxidizes YZ on the nanosecond time scale.¹⁶ If YD is available to act as an electron donor, i.e. after long dark adaptation, YD is also oxidized on the nanosecond time regime by P_{680}^+ .¹⁷ YZ^\bullet is reduced by the OEC with a

microsecond–millisecond rate, which depends on S state.¹⁸ The S_1 to S_2 transition has a half-inhibition temperature of 135 K, while the S_0 to S_1 , S_2 to S_3 , and S_3 to S_0 transitions occur at 220–235 K.¹⁹ Thus, at 190 K, the S_2 to S_3 transition cannot occur. Acceptor side quinone molecules, Q_A and Q_B , act as electron acceptors. At 190 K, PSII is limited to one charge separation; Q_B is not functional.²⁰ EPR signals from the neutral radicals,²¹ YD^\bullet and YZ^\bullet , can be measured and distinguished by their decay kinetics^{22,23} and by their microwave power dependence in the presence of the OEC.²⁴

In many previous studies of YZ PCET, the OEC was removed or was absent due to biochemical manipulation of PSII. Removal of the OEC slows YZ^\bullet reduction.²⁵ However, removal of the OEC may influence YZ PCET reactions by a conformational change or by a change in hydrogen bonding (Figure 1B). Recently, high-field EPR spectroscopy suggested that there is no change in YZ^\bullet g tensor orientation when crystals of PSII and OEC depleted PSII were compared.²⁶

In this work, YZ^\bullet PCET was studied in the presence of the OEC. Oxygen-evolving PSII samples were prepared in the S_1 state by dark adaptation and then illuminated at 190 K to give the S_2 state. A saturating 532 nm flash was then used to generate $S_2YZ^\bullet Q_A^-$. The S_2 state cannot act as an electron donor at this temperature, and therefore, YZ^\bullet decays by recombination with Q_A . The rate of the $P_{680}^+ Q_A^-$ reaction is on the microsecond time scale in plant PSII and is pH and solvent isotope insensitive {see refs 27 and 28}. The YZ^\bullet and Q_A^- recombination reaction occurs on a much longer time scale, with an overall time constant of 100–500 ms in the absence of the OEC.^{23,29} In the presence of the OEC, the rate of YZ^\bullet and Q_A^- recombination was similar with reported $t_{1/2}$ values of 9.5 s (27%) and 0.8 s (73%) (pH 6.5, 190 K).²⁴

A representative field sweep spectrum of YZ^\bullet in the S_2 state at 190 K is shown in Figure 2A. Q_A^- gives rise to a spin-coupled signal with an acceptor side Fe^{2+} ion and is not detectable under these conditions.³⁰ The decay of YZ^\bullet was monitored by changes in EPR intensity at a fixed magnetic field (Figure 2A, arrow). Secondary electron donors, such as chl, carotenoid, and cytochrome $b559$, are not observed at this field position and temperature.^{31–34} The use of high microwave power saturates the YD^\bullet signal.²⁴ As expected, the g value of the YZ^\bullet radical is 2.004.^{21,35} The YZ^\bullet spectrum and decay kinetics are similar to a previous report.²⁴

In Figure 3B, the YZ^\bullet decay kinetics were monitored, the data were fit, and the overall half-time as a function of p^1H was plotted (black line). For comparison, the half-times for YD^\bullet decay were derived from published rate constants for the majority phase,¹⁵ which are plotted in Figure 3A. While the rate of YD^\bullet decay accelerates by a factor of 10 at low p^1H (Figure 3A), YZ^\bullet decay did not show significant pH dependence (Figure 3B, black line) in $^1\text{H}_2\text{O}$ buffers. YZ^\bullet decay showed only a modest pH dependence in $^2\text{H}_2\text{O}$ buffers (Figure 3B, red line). This difference may not be significant, given the error, which is estimated as one standard deviation. Over this pH range, the steady state rate of oxygen evolution was constant, and the content of extrinsic polypeptides was similar. Higher pL values led to activity loss and depletion of the extrinsic polypeptides (data not shown).

The solvent isotope effect was calculated from the data in Figure 3B. Figure 3C shows the YZ^\bullet solvent isotope effect as a function of pL. A significant solvent isotope effect was observed from pL 5.0 to 7.5 with an average value of ~ 2 . The value of the solvent isotope effect is pH independent, given the standard

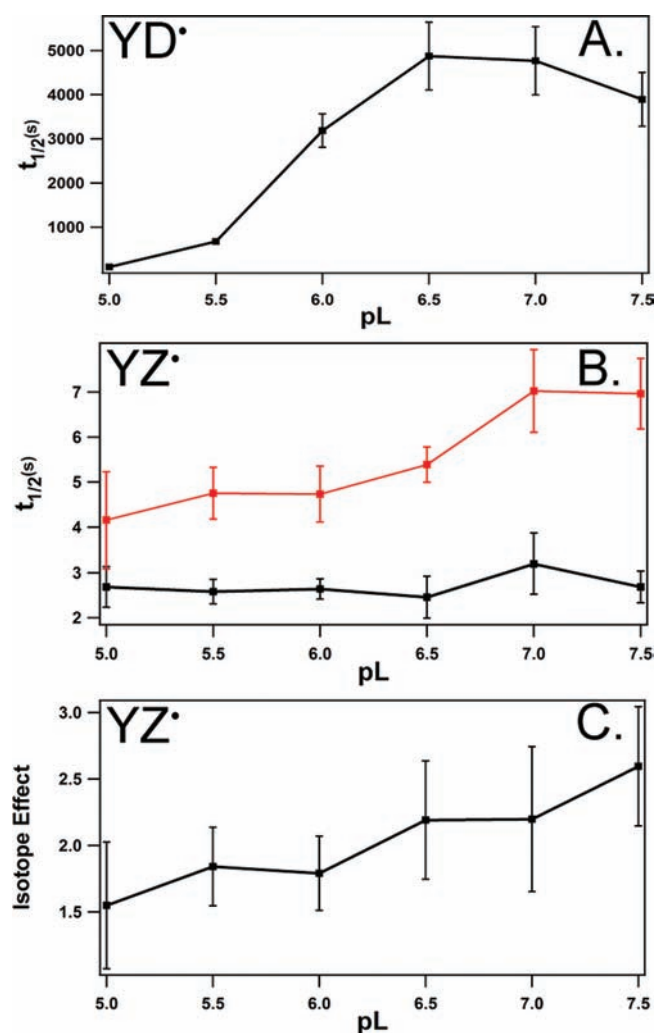


Figure 3. (A) pL dependence of YD^\bullet decay, as assessed by EPR spectroscopy, attributed to $\text{YD}^\bullet\text{Q}_\text{A}^-$ recombination, and derived from ref.¹⁵ For pH 5.5 to 7.5, the half-life was derived from the rate constant for the majority phase, corresponding to >85% of the amplitude. For pH 5.0, the data were fit with a single exponential. (B) pL dependence of YZ^\bullet recombination in the S_2 state at 190 K. Data were acquired either in $^1\text{H}_2\text{O}$ (black) or $^2\text{H}_2\text{O}$ (red) buffers. (C) pL dependence of the solvent isotope effect for YZ^\bullet recombination, derived from the data in (B).

deviations. The overall magnitude is consistent with a pH-independent, kinetic isotope effect (KIE) on YZ^\bullet recombination with Q_A^- . The observation of a significant solvent isotope effect between pL 5.0 and 7.5 implies that the YZ pocket is exposed and readily accessible to water, consistent with recent X-ray crystal structures.^{4,5} Thus, the lack of pH dependence (Figures 3B and C) cannot be attributed to lack of accessibility. By contrast, the decay of YD^\bullet showed a ~ 10 -fold increase in rate at low pH (Figure 3A) and a pH-dependent isotope effect, with a maximum value of 2.4 at high pL.¹⁵ A proton inventory at high pL was consistent with multiple proton transfer pathways to YD^\bullet , with histidine and water molecules suggested to be the proton donors on the two different pathways.³⁶

Phenol and tyrosine model compounds have been used to determine the mechanism of PCET reactions. PCET may occur through a concerted pathway, in which the electron and proton are transferred in one kinetic step and through one transition

state (CPET). Alternatively, either the electron or proton may be transferred first (defined as ETPT or PTET, respectively). In tyrosine model compounds, a CPET mechanism has been inferred in some studies.^{37–40} The magnitude of the KIE and the pH dependence can be used as a first approach to distinguish these mechanisms.

For YD^\bullet reduction, the pH dependence and the kinetic isotope effect were used to argue that the mechanism is PTET at low pH and CPET at high pH.³⁶ Unlike YD^\bullet , YZ^\bullet recombination does not show an increased rate at low pH values. The lack of significant pH dependence is not consistent with a PTET mechanism.^{38,40} The observation of a significant (average 2.0) kinetic isotope effect is not consistent with an ETPT mechanism.^{38,40} In refs 38 and 40, an isotope effect of 1.6 or greater was considered to be consistent with CPET. In ref 41, CPET in model phenols with internal hydrogen bonding was pH independent, and in ref 40, CPET in model phenols in neat water was pH independent at low pH values. Therefore, our data are consistent with a CPET mechanism for YZ^\bullet reduction. The experiments also suggest that PCET mechanisms distinguish YD and YZ .

The experiments presented here focus on the mechanism of YZ^\bullet reduction. Previous work has been concerned with the mechanism of YZ oxidation. For OEC-depleted preparations, optical studies of P_{680}^+ reduction were used to argue a CPET mechanism at low pH and a pure ET or a PTET mechanism at high pH.^{37,42} A pK of ~ 7.5 was derived from the optical data and attributed to titration of a base near YZ . As shown in Figure 1, removal of the OEC may influence PCET reactions. For OEC-containing preparations, optical studies of P_{680}^+ reduction have provided no significant solvent isotope effect on nanosecond components of this reaction.^{43–45} This is in contrast with our results on the reduction reaction. A significant equilibrium isotope effect⁴⁶ may explain a difference in KIE on the oxidation and reduction reactions. Low fractionation factors can occur if YZ is involved in a strong hydrogen bond, in which case deuterium will prefer the solvent.⁴⁷

Model compound studies have shown that intermolecular and intramolecular hydrogen bonds facilitate CPET reactions.^{37–40,48,49} These reactions avoid the formation of high-energy intermediates but occur at the expense of a high reorganization energy, which is defined as the energy to reorganize from the initial to final coordinates, without charge transfer.^{37–40} We propose that the extensive hydrogen-bonding network around YZ^\bullet and the calcium ion facilitates CPET at low pH.⁵ In the 1.9 Å structure, His 190 is located 2.5 Å from YZ and several water molecules, bound to calcium, are modeled with one water at 2.6 Å (Figure 1B). The observation that recombination of YZ^\bullet is not accelerated at low pH is of significance with regard to PSII activity, which must be maintained under the acidic conditions of the thylakoid lumen.

AUTHOR INFORMATION

Corresponding Author

bridgette.barry@chemistry.gatech.edu

ACKNOWLEDGMENT

This work was supported by NIH GM43273 (NIGMS and NEI) to B.A.B.

REFERENCES

(1) Joliet, P.; Kok, B. In *Bioenergetics of Photosynthesis*; Govindjee, Ed.; Academic Press: New York, 1975; pp 387–412.

- (2) Barry, B. A.; Babcock, G. T. *Proc. Natl. Acad. of Sci. U.S.A.* **1987**, *84*, 7099–7103.
- (3) Boerner, R. J.; Barry, B. A. *J. Biol. Chem.* **1993**, *268*, 17151–17154.
- (4) Guskov, A.; Kern, J.; Gabdulkhakov, A.; Broser, M.; Zouni, A.; Saenger, W. *Nat. Struct. Mol. Biol.* **2009**, *16*, 334–342.
- (5) Umena, Y.; Kawakami, K.; Shen, J.-R.; Kamiya, N. *Nature* **2011**, *473*, 55–60.
- (6) Debus, R. J.; Barry, B. A.; Sithole, I.; Babcock, G. T.; McIntosh, L. *Biochemistry* **1988**, *27*, 9071–9074.
- (7) Metz, J. G.; Nixon, P. J.; Rögner, M.; Brudvig, G. W.; Diner, B. A. *Biochemistry* **1989**, *28*, 6960–6969.
- (8) Debus, R. J.; Barry, B. A.; Babcock, G. T.; McIntosh, L. *Proc. Natl. Acad. of Sci. U.S.A.* **1988**, *85*, 427–430.
- (9) Vermaas, W. F. J.; Rutherford, A. W.; Hansson, Ö. *Proc. Natl. Acad. of Sci. U.S.A.* **1988**, *85*, 8477–8481.
- (10) Ananyev, G. M.; Sakiyan, I.; Diner, B. A.; Dismukes, G. C. *Biochemistry* **2002**, *41*, 974–980.
- (11) Barry, B. A. *J. Photochem. Photobiol., B* **2011**, *104*, 60–71.
- (12) Boussac, A.; Etienne, A. L. *Biochim. Biophys. Acta* **1984**, *766*, 576–581.
- (13) Berthold, D. A.; Babcock, G. T.; Yocum, C. F. *FEBS Lett.* **1981**, *134*, 231–234.
- (14) Barry, B. A. *Methods Enzymol.* **1995**, *258*, 303–319.
- (15) Jenson, D.; Evans, A.; Barry, B. A. *J. Phys. Chem. B* **2007**, *111*, 12599–12604.
- (16) Gerken, S.; Brettel, K.; Schlodder, E.; Witt, H. T. *FEBS Lett.* **1988**, *237*, 69–75.
- (17) Faller, P.; Debus, R. J.; Brettel, K.; Sugiura, M.; Rutherford, A. W.; Boussac, A. *Proc. Natl. Acad. of Sci. U.S.A.* **2001**, *98*, 14368–14373.
- (18) Babcock, G. T.; Blankenship, R. E.; Sauer, K. *FEBS Lett.* **1976**, *61*, 286–289.
- (19) Styring, S.; Rutherford, A. W. *Biochim. Biophys. Acta* **1988**, *933*, 378–387.
- (20) de Paula, J. C.; Innes, J. B.; Brudvig, G. W. *Biochemistry* **1985**, *24*, 8114–8120.
- (21) Barry, B. A.; El-Deeb, M. K.; Sandusky, P. O.; Babcock, G. T. *J. Biol. Chem.* **1990**, *265*, 20139–20143.
- (22) Kim, S.; Barry, B. A. *Biochemistry* **1998**, *37*, 13882–13892.
- (23) Ayala, I.; Kim, S.; Barry, B. A. *Biophys. J.* **1999**, *77*, 2137–2144.
- (24) Ioannidis, N.; Zahariou, G.; Petrouleas, V. *Biochemistry* **2008**, *47*, 6292–6300.
- (25) Babcock, G. T.; Sauer, K. *Biochim. Biophys. Acta* **1975**, *376*, 315–28.
- (26) Matsuoka, H.; Shen, J.-R.; Kawamori, A.; Nishiyama, K.; Ohba, Y.; Yamauchi, S. *J. Am. Chem. Soc.* **2011**, *133*, 4655–4660.
- (27) Diner, B. A.; Force, D. A.; Randall, D. W.; Britt, R. D. *Biochemistry* **1998**, *37*, 17931–17943.
- (28) de Wijn, R.; van Gorkom, H. J. *Biochemistry* **2001**, *40*, 11912–11922.
- (29) Dekker, J. P.; van Gorkom, H. J.; Brok, M.; Ouweland, L. *Biochim. Biophys. Acta* **1984**, *764*, 301–309.
- (30) Rutherford, A. W.; Zimmermann, J. L. *Biochim. Biophys. Acta* **1984**, *767*, 168–175.
- (31) MacDonald, G. M.; Boerner, R. J.; Everly, R. M.; Cramer, W. A.; Debus, R. J.; Barry, B. A. *Biochemistry* **1994**, *33*, 4393–4400.
- (32) MacDonald, G. M.; Steenhuis, J. J.; Barry, B. A. *J. Biol. Chem.* **1995**, *270*, 8420–8428.
- (33) Buser, C. A.; Diner, B. A.; Brudvig, G. W. *Biochemistry* **1992**, *31*, 11449–11459.
- (34) Hanley, J.; Deligiannakis, Y.; Pascal, A.; Faller, P.; Rutherford, A. W. *Biochemistry* **1999**, *38*, 8189–8195.
- (35) Ayala, I.; Range, K.; York, D.; Barry, B. A. *J. Am. Chem. Soc.* **2002**, *124*, 5496–5505.
- (36) Jenson, D.; Barry, B. A. *J. Am. Chem. Soc.* **2009**, *131*, 10567–10573.
- (37) Sjödin, M.; Styring, S.; Akermark, B.; Sun, L.; Hammarström, L. *J. Am. Chem. Soc.* **2000**, *122*, 3932–3936.
- (38) Mayer, J. M.; Rhile, I. J. *Biochim. Biophys. Acta* **2004**, *1655*, 51–58.
- (39) Irebo, T.; Reece, S. Y.; Sjödin, M.; Nocera, D. G.; Hammarström, L. *J. Am. Chem. Soc.* **2007**, *129*, 15462–15464.
- (40) Bonin, J.; Costentin, C.; Louault, C.; Robert, M.; Routier, M.; Savéant, J.-M. *Proc. Natl. Acad. of Sci. U.S.A.* **2010**, *107*, 3367–3372.
- (41) Sjödin, M.; Irebo, T.; Utas, J. E.; Lind, J.; Merényi, G.; Akermark, B.; Hammarström, L. *J. Am. Chem. Soc.* **2006**, *128*, 13076–13083.
- (42) Rappaport, F.; Boussac, A.; Force, D.; Pelloquin, J.; Bryndal, M.; Sugiura, M.; Un, S.; Britt, D.; Diner, B. *J. Am. Chem. Soc.* **2009**, *131*, 4425–4433.
- (43) Karge, M.; Irrgang, K.-D.; Renger, G. *Biochemistry* **1997**, *36*, 8904–8913.
- (44) Haumann, M.; Bogershausen, O.; Cherepanov, D.; Ahlbrink, R.; Junge, W. *Photosynth. Res.* **1997**, *51*, 193–208.
- (45) Schilstra, M. J.; Rappaport, F.; Nugent, J. H. A.; Barnett, C. J.; Klug, D. R. *Biochemistry* **1998**, *37*, 3974–3981.
- (46) Schowen, K. B.; Schowen, R. L. *Methods Enzymol.* **1982**, *87*, 551–606.
- (47) Cleland, W. W. *Biochemistry* **1992**, *31*, 317–319.
- (48) Hammes-Schiffer, S.; Soudackov, A. V. *J. Phys. Chem. B* **2008**, *112*, 14108–14123.
- (49) Irebo, T.; Johansson, O.; Hammarström, L. *J. Am. Chem. Soc.* **2008**, *130*, 9194–9195.